NOLTR 70-133

HYDRODYNAMIC BEHAVIOR OF HBX-1 AND EQUATION OF STATE OF THE DETONATION PRODUCTS BELOW THE CHAPMAN-JOUGUET STATE

By
L. A. Roslund
N. L. Coleburn

6 November 1970

NOL

UNITED STATES NAVAL ORDNANCE LABORATORY, WHITE OAK, MARYLAND

NOLTR 70-133

NOLTR 70-133

HYDRODYNAMIC BEHAVIOR OF HBX-1 AND EQUATION OF STATE OF THE DETONATION PRODUCTS BELOW THE CHAPMAN-JOUGUET STATE

by:

L. A. Roslund

and

N. L. Coleburn

ABSTRACT: The stability to detonation and the expansion behavior of reaction products were studied for an aluminized explosive, HBX-1. The detonation velocity-charge diameter and detonation velocity-loading density relationships were determined by streak camera techniques and electronic probe methods. These data gave reaction zone lengths which increase from 0.07 mm for an initial explosive density of 1.72 g/cm^3 to 1.5 mm at 1.3 g/cm^3. With the pressure-particle velocity relation established from 338,000 bars to 15 bars, and conditions in the C-J state (P_{CJ} = 220.4 kbars) specified, the generalized hydrodynamic relations derived by Jones were used to evaluate the constants in an empirical equation of state and in the Wilkins equation of state as modified by Allan and Lambourn.

PUBLISHED 6 NOVEMBER 1970

Explosion Dynamics Division
Explosions Research Department
U.S. Naval Ordnance Laboratory
White Oak, Silver Spring, Maryland

NOLTR 70-133 6 November 1970

HYDRODYNAMIC BEHAVIOR OF HBX-1 AND EQUATION OF STATE OF THE DETONATION PRODUCTS BELOW THE CHAPMAN-JOUGUET STATE

This report presents measured detonation parameters of an aluminized explosive, HBX-1, and describes the expansion behavior of HBX-1 explosion products. An empirical equation-of-state for HBX-1 detonation products is obtained. This work should be of special interest to workers involved in analyses and prediction of explosion effects. The work was supported by ORD Task No. ORD 332 001/UF17 354 315, Problem 201, Explosives Underwater Research and Technology.

GEORGE G. BALL
Captain, USN
Commander

C. J. ARONSON
By direction

CONTENTS

TABLES

FIGURES

I. INTRODUCTION

1. The detonation of an explosive produces flow in the surrounding medium which is directly affected by the way the available energy is released as the reaction products expand to low pressures. The energy released is from the work integral

$$A = \int_{V_o}^{V} PdV = Q - q \qquad (1)$$

where A is the maximum available work in an adiabatic expansion of the detonation products from the initial explosive volume V_o, to the final specific volume V at pressure P. Q is the heat of detonation and q is the heat retained by the detonation products at V.

2. Calculations of the maximum work from Eq. (1) are handicapped because little is known about the detonation reactions or the characteristics of the pressure-volume expansion adiabat. Many attempts have been made to develop more elaborate equations of state for the detonation reaction products. The results of Deal* and considerations by Fickett and Wood[2] seemed to support the view that for some explosives a constant gamma adiabat may adequately describe the product gas expansion states. However, energy transfer computations using the constant gamma assumption indicate the assumption is incorrect, since the results are in considerable disagreement with experimental measurements from metal acceleration experiments. Moreover the assumption is not expected to describe the expansion behavior of burnt gases from explosive compositions with substantial after-burning reactions.

3. In this work we studied the hydrodynamic behavior of the detonation products from an aluminized explosive, HBX-1, by making measurements of the pressure-particle velocity relationship for its C-J adiabat. With these data we have described the expansion behavior from 338,000 bars to 15 bars, using a characteristic form of the Wilkins equation of state (2a) as modified by Allan and Lambourn[3] and an empirical equation of state (2b). These equations are:

*References are on page 13.

$$P = \begin{cases} B \exp(-kV) + WG_1 V^{-(1+W)} & V \leq V_C \quad (2a) \\ G_2 (V + V^*)^{-1} & V > V_C \quad (2b) \end{cases}$$

where V_C is a critical volume which specifies the properties of the adiabat. In regions of high pressure with volumes less than V_C our data are best fitted by the first equation and in regions of expansion for volumes greater than V_C our data obey the second equation. B, k, G_1, W, G_2, and V^* are constants. The following sections describe how the experimental determination of the hydrodynamic properties is used in evaluating the equation-of-state constants. These properties are the change in the infinite diameter value of the detonation velocity with loading density, the properties of the C-J state, and experimental P-u data for an expansion from the C-J state. The expansion adiabat derived from these data is compared with the constant gamma isentrope PV^γ = constant, and the variation of $\gamma = -\left(\frac{\partial \ln P}{\partial \ln V}\right)_S$ with volume is calculated.

II. EXPERIMENTAL ARRANGEMENTS AND RESULTS

Charge Preparation

4. The explosive configuration used in the experiments was a cylindrical charge of pressed HBX-1, RDX/TNT/Aluminum/WAX (40/38.1/17.1/4.8) by weight, which was initiated by a plane-wave explosive system. The pressed charges* were prepared by mixing granular RDX and TNT into a mixture of 18 parts aluminum and 5 parts wax by weight. This mixture was formed by stirring aluminum and Stanolind wax in carbon tetrachloride and then evaporating the solvent. Seventy percent of the HBX-1 by weight consisted of material (aluminum, RDX, and TNT) with particle sizes between 44 microns and 180 microns. Charges with particle sizes in this range were formed at the desired charge density in a hydrostatic press and then machined to the appropriate dimensions.

Detonation Velocity Measurements and Results

5. Detonation velocities and the critical diameter of HBX-1 were measured as a function of charge density using smear camera and "raster oscilloscope" pin techniques. In the smear camera measurements, unconfined HBX-1 at loading densities ranging from about 1.33 g/cm^3 (75% TMD**) to about 1.74 g/cm^3 (98% TMD) was detonated in a "stacked" cylinder configuration. This configuration consisted of five explosive cylinders of different diameters but of the same loading density. The cylinders were stacked in order of decreasing diameters; 5.08-cm, 2.54-cm, 1.27-cm, 0.635-cm, and 0.476-cm. The cylinder heights corresponding to these diameters were 10.2-cm, 10.2-cm, 5.08-cm, 3.81-cm, and 3.81-cm, respectively. The stacked cylinders were fired by the detonation of a tetryl booster 5.08-cm diameter by 2.54-cm high. The tetryl was initiated by a 5.08-cm diameter pentolite-baratol plane-wave booster. Techniques described in reference 4 were used to give narrow, bright light pips which facilitated the analysis of the detonation trace on the smear camera records. The failure diameter for each charge density was estimated by examining the smear camera record for the diameter at which the detonation wave failed to propagate with a steady velocity. Single charges each 37-cm long, 5.08-cm diameter and

* Cast charges also were fired to compare their diameter effect with pressed charges at the highest experimental density, about 1.74 g/cm^3.
** Theoretical maximum density, 1.76 g/cm^3.

2.54-cm diameter also were fired simultaneously with the stacked cylinder array and the detonation velocities were measured using electronic probes and a raster-type oscilloscope. In these measurements the circuit consisted of a single strip of copper running the length of the charge, separated by an air gap from a series of electrically-charged precisely spaced copper strips which served as probe contacts to be consecutively shorted by the passage of the shock.

6. The camera data (which was less precise) generally showed agreement with the probe data to better than 0.5%. The electronic measurements were precise to better than ±0.2%. With this precision in the velocity measurements, the greatest source of error in the experiments probably is the density variation within the test explosive.

7. Examination of the detonation traces from the stacked cylinder array showed that detonation did not propagate into the 0.476-cm diameter charges. The critical minimum diameter for HBX-1 is about 0.6 cm. From the measurements, we determined a critical density (between 1.602 g/cm^3 and 1.530 g/cm^3) below which detonation will not propagate in pressed HBX-1 at about 0.6-cm diameter. We infer that detonation cannot occur in smaller diameters at densities lower than this critical density[5]. Moreover, we found a sharply different sensitivity between pressed and cast HBX-1. For example, charges of 0.635-cm diameter pressed to 1.72 g/cm^3 detonated; cast charges of the same density and diameter failed.

8. The detonation velocities for charges loaded at various densities in the different charge diameters are plotted in Fig. 1. Linear least square lines are drawn through the data. The effect of charge diameter on the velocities is greatest at lower loading densities. We extrapolated the curves relating the measured detonation velocity to the reciprocal of the charge diameter for different loading densities. For charge diameters $\geq$1.27 cm the curves appear linear. The extrapolation gave the velocities, D_∞, for the infinite diameter or ideal curve which is represented by

$$D_\infty = -0.063 + 4.305\ \rho \quad . \qquad (3)$$

9. The curved front theory[4] relates D_∞, the reaction zone length a, and the charge diameter d, to the detonation velocity D,

$$D = D_\infty\ (1 - a/d) \quad . \qquad (4)$$

Assuming the equation only applies to charge diameters >1.27 cm, we computed values of the reaction zone lengths which are plotted as functions of density in Fig. 2. The result is a smooth decrease of the reaction zone length with increasing density. This result is

attributed to grain size reduction caused by the crushing action of compaction to higher density. Smaller grain size means more material surface exposed to initiation and hence faster reaction.

10. Wood and Kirkwood[7] give a relation between reaction zone length and curvature of the detonation front,

$$a = (R/3.5)(1 - D/D_\infty) \quad , \tag{5}$$

where R is the radius of curvature of the detonation front. Extensive studies of the shape of the wave by Cook, et al[8], show the front is spherical. Hence, maximum curvature, i.e., minimum radius, is likely at the critical diameter

$$R = \frac{1}{2} d_c \quad . \tag{6}$$

At the critical diameter, 0.635 cm, and critical density, about 1.60 g/cm^3, the measured detonation velocity is 5234 m/sec, and D_∞ = 6820 m/sec. These data give a reaction zone length of 0.21 mm as compared to 0.40 mm from Fig. 2.

Shock Impedance Measurements of the Chapman-Jouguet State

11. The pressure and specific volume of the explosion products centered at the C-J state were determined from shock wave velocity or free-surface velocity measurements, using equation-of-state data from several sources.* Shock waves were transmitted into several materials of various specified thicknesses in contact with detonating HBX-1 and the above parameters were measured (Table I). To denote the attenuation and narrow limits of the von Neumann spike region[9], the data from these experiments were linearly extrapolated to values for zero thickness.

12. For these shock wave measurements the charge configuration consisted of a 12.7-cm diameter, 6.4-cm high cylinder of HBX-1, initiated on one end face by an explosive plane-wave lens of the same diameter. The other face of the cylinder was held in close contact with the inert material using a thin silicone-grease film to eliminate air gaps. Measurements of the free-surface velocities and shock wave velocities were made for various plate and wedge thicknesses of aluminum, brass, Plexiglas, and polyurethane which were shocked by detonating HBX-1 in the above charge geometry. A reflected-light smear camera technique described previously[10] was used for these measurements. The initial shock wave velocity in water was measured from the end face of an HBX-1 cylinder 5.08-cm diameter and 15-cm long.

13. The C-J isentrope behavior from about 20 kbars to 15 bars was determined from optical measurements of the initial velocities of shock waves produced by detonating HBX-1 in air and argon initially at compressed or reduced pressure states. These experiments were done in an expendable, gas-tight chamber which could be filled

*See Table II for equation-of-state references for the various materials.

with compressed gas at 1000 psi or evacuated to about 0.01 bar. Figure 3 shows the experimental arrangement. The chamber consisted of a 7.62-cm inside diameter, 26-cm long cast iron pipe tee, with 0.5-cm thick walls. The opposite ends of the pressure chamber tee were fitted with 2.54-cm thick Plexiglas windows to allow viewing of the charge configuration with a rotating-mirror smear camera. The bottom end of the chamber was covered by a brass plate designed to give an air-tight seal and also to transfer detonation from a detonator outside the chamber to a plane-wave initiator inside the chamber.

14. The charges fired in the chamber were 5.08-cm diameter cylinders, 16.5-cm long and were confined in copper cylinders with 0.64-cm thick walls. This confinement sufficiently reduces the diameter effect on HBX-1 so that the shock velocity data are considered applicable to an ideal charge. For viewing purposes, one end face of the explosive protruded about 1.27 cm from the copper cylinder. The other end face of the HBX-1 was initiated by an explosive train consisting of a 2.54-cm long, 5.08-cm diameter pentolite pellet, a pentolite-baratol plane-wave generator and an SE-1 detonator.

15. The slit of the smear camera was aligned to view the shock wave emerging from the protruding face of the charge for a distance of one charge radius, about 2.54 cm. Figure 4 shows the shock wave trace emerging from a detonating charge in air initially at 0.00355 g/cm^3. The camera writing speed was 3.8 mm/usec. The shock wave velocity was determined from the distance vs. transit time readings of the trace. Vertical distance on the film was converted to laboratory coordinates using magnification reference markers positioned inside the test chamber.

16. In the region 1 mm to 6 mm from the charge surface, the trace readings gave velocities which were characteristically high and not reproducible. This was attributed to "fog over" from intense shock light on the record, or possible blow-off of luminous detonating particles from the charge surface. The region 6 mm to 20 mm from the charge gave trace readings which were essentially linear. Slope measurements were made in this region to obtain the initial gas shock velocities.

17. We used the data in reference 11 to calculate shock pressures and particle velocities corresponding to our measured air shock velocities. Since our measured shock velocities in argon are in the range of the shock Hugoniot of argon determined by Christian, Duff, and Yarger[12], we used their relation for the particle velocities in Table II. We obtained good support for these data from the calculations by Bond[13] of the shock Hugoniots of argon for several initial pressures.

III. EXPERIMENTAL DATA ANALYSIS

18. We obtained the data in Table II from the measured shock wave velocities and free-surface velocities corresponding to zero thickness of the various solid materials and their known shock Hugoniots. Since the pressures and particle velocities are continuous across the reaction products-material interface, the P-u data correspond to points on the detonation products Hugoniot above the C-J state and on the expansion adiabat below the C-J state. The P-u data are plotted in Fig. 5.

19. To establish the C-J state we assumed that the aluminum and wax in HBX-1 are chemically and physically inert in the detonation front[14]. The detonation parameters then are functions of the nominal density, ρ_o of the explosive components in the charge, i.e., the ratio (weight of explosive)/(volume available to the explosive). For HBX-1 with the experimental charge density of 1.712* g/cm^3, we obtain ρ_o = 1.624 g/cm^3.

20. The C-J state was established according to the impedance match conditions by drawing the straight line with slope, $\rho_o D = P/u$ through the origin to intersect the curve given by an exponential fit to the P-u data above 10 kbar. With D = 7307 m/sec we obtain P_{CJ} = 220.4 kbars, u_{CJ} = 1858 m/sec. Then using the detonation theory, at the C-J point

$$D = u_{CJ} + C \tag{7}$$

where C is the velocity of sound at the C-J point. The isentropic exponent

$$\gamma_{CJ} = (\rho_o D^2/P_{CJ}) - 1 \quad . \tag{8}$$

Also

$$\rho_{CJ}/\rho_o = \frac{D}{D - u_{CJ}} \tag{9}$$

and for the experimental C-J point, ρ_{CJ} = 2.178 g/cm^3 and γ = 2.934.

*This density is typical for HBX-1 in warhead applications.

21. The constants in the characteristic equation of state, Eq. (2a), were evaluated from the experimental data, following the generalized formulation of the detonation theory by Jones[15]. Jones defines the quantity α, from the detonation products Hugoniot by

$$\frac{\partial (E - \Omega)_P}{\partial V} = \frac{P}{\alpha} \quad , \tag{10}$$

where E is the internal energy of the detonation products. We assume no radial expansion at the C-J plane. Therefore, α is evaluated from the infinite diameter detonation velocity-loading density relation, Eq. (3) and γ_{CJ}, the initial value of the isentropic exponent in

$$\gamma = - \left(\frac{\partial \log P}{\partial \log V}\right)_S \quad . \tag{11}$$

As given by Jones, (reference 15, Eq. (14))

$$\alpha = (\gamma_{CJ} + 1)/\left(1 + \frac{\rho_o dD}{D d\rho_o}\right) - 2 \quad . \tag{12}$$

Following Allan and Lambourn's formulation, the constant W in the equation of state

$$P = B \exp(-kV) + WG_1 V^{-(1 + W)}$$

for $V \leq V_C$ was found from

$$W = \alpha\gamma_{CJ}/(\alpha + 1) \quad . \tag{13}$$

B and G_1 were determined from Eq. (2a) and Eq. (11) using the C-J values of P, V, and γ. Differentiation of Eq. (2a) with respect to V gives

$$-\frac{dP}{dV} = kB \exp(-kV) + W(1 + W)G_1 V^{-(2+W)} \quad . \tag{14}$$

Also, Eq. (11) gives

$$-\frac{dP}{dV} = \frac{\gamma P}{V} \quad . \tag{15}$$

With $\rho = V^{-1}$ and the C-J values one then obtains

$$G_1 = \frac{P_{CJ}(\gamma_{CJ}\rho_{CJ} - k)\rho_{CJ}^{-(1 + W)}}{W[(1 + W)\rho_{CJ} - k]} \quad , \tag{16}$$

and

$$B = [P_{CJ} - WG_1\rho_{CJ}^{(1+W)}] \exp(k/\rho_{CJ}) \quad . \tag{17}$$

22. Then a value of k was chosen to give the best fit to the experimental P-u adiabat in the region $V < V_C$. To calculate the P-u adiabat from the characteristic equation we used the Riemann relation

$$u - u_1 = \int_{\rho_1}^{\rho} C \frac{d\rho}{\rho} \tag{18}$$

where C is the velocity of sound; u_1 and ρ_1 are the particle velocity and density for our known state, in this case the C-J state. For the adiabat, C is given by

$$C = \left(\frac{\partial P}{\partial \rho}\right)_S^{1/2} = V\left(-\frac{\partial P}{\partial V}\right)_S^{1/2} \quad . \tag{19}$$

23. In the region where $V > V_C$ the empirical equation is $P = G_s/(V+V^*)$. This follows since in Fig. 5, the experimental P-u data in the lower region are related best by

$$\log P = Mu + A \quad , \tag{20}$$

where M and A are constants determined from the experimental data. Differentiation of Eq. (18) and Eq. (20) gives, with Eq. (19),

$$\left(\frac{du}{dV}\right)^2 = -\frac{dP}{dV} \tag{21}$$

$$\frac{dP}{du} = MP \tag{22}$$

$$\frac{du}{dV} \cdot \frac{dV}{dP} = \frac{1}{MP} \tag{23}$$

$$\left(\frac{1}{MP}\right)^2\left(\frac{dP}{dV}\right)^2 = -\frac{dP}{dV} \tag{24}$$

$$-\frac{dP}{P^2} = M^2 dV \quad . \tag{25}$$

Since the reference state is now the critical point with the characteristic values P_C and V_C, we have

$$-\int_{P_c}^{P} \frac{dP}{P^2} = \int_{V_c}^{V} M^2 dV \qquad (26)$$

$$\frac{1}{P} - \frac{1}{P_c} = M^2(V - V_c) \qquad (27)$$

$$P[V - V_c + 1/(P_c M^2)] = 1/M^2 \quad . \qquad (28)$$

With

$$V^* = -V_c + 1/(P_c M^2) \text{ and } G_2 = 1/M^2 \quad , \qquad (29)$$

we then have

$$P(V + V^*) = G_2 \quad . \qquad (30)$$

V_c is evaluated by iteration, using Eq. (18) to calculate the P-u adiabat from Equations (2a) and (2b) and then comparing the results with the experimental data of Fig. 5. P_c is calculated from the characteristic equation using $V = V_c$. Equation (29) gives the value of V^*.

IV. DISCUSSION

24. The equation of state constants for HBX-1 are listed in Table III. The small values of α and W are typical for explosive compositions with large amounts of solid or non-ideal detonation products as indicated by the relatively large values of $dD/d\rho_o$. For pure explosives, α varies from about 0.2 to 0.8, depending on the loading density, and $dD/d\rho_o$ ranges from about 3000 to 3500 $\frac{m}{sec}/\frac{g}{cm^3}$.

25. The "best fit" to the experimental P-u data for $V < V_C$ is obtained with the parameter $k = 6.45$ g/cm^3; $B = 4.187$ Mbar and $G_1 = 0.00397$ Mbar in the characteristic equation (Eq. (2a). The experimental P-u relation for $V > V_C$ gives $M = -10.4589$ μsec/cm, $G_2 = 9.142 \times 10^9$ (cm/sec)^2. The solid line in Fig. 5 is obtained when $V_C = 1.15$ cm^3/g then $P_C = 3.645$ kbar and $V^* = 1.358$ cm^3/g.

26. If the complete P-u adiabat is calculated using the modified Wilkins equation for $V > V_C$, the curve deviates from the experimental data as shown in Fig. 5. Also plotted in Fig. 5 is the constant γ adiabat P-u curve. The experimental P-u data from 20 kbars to 1 kbar are well below this curve. This covers the range of the compressed gas experiments. We note an abrupt upward trend in the particle velocity data at about 10 kbars. The trend is considered real and not a result of experimental error. At points below 1 kbar the experimental data shift significantly away from the constant γ curve. These data result from the detonation products expanding into a rarefied atmosphere, i.e., the initial conditions of the reduced pressure experiments.

27. The pressure-volume adiabats for the characteristic and empirical equation of state. the modified Wilkins equation, and the constant gamma "straight line" assumption are shown in Fig. 6. The adiabat derived from the experimental data dips below the constant gamma curve near the C-J point and then crosses over both the constant gamma and modified Wilkins equation of state curves below 3 kbars. The inflection in our experimental data beginning at about 3.0 kbars produces the sharp break in the adiabat at $V = 1.15$ cm^3/g. The variation of $\gamma = -\left(\frac{\partial \ln P}{\partial \ln V}\right)_S$ with volume for the modified Wilkins equation of state is shown in Fig. 7. We note that γ first increases from its C-J value of 2.934, to about 3.9, and finally decreases to 1.343. This final value is compatible with the value of W in the equation of state, i.e., the limiting value, $\gamma = 1 + W$.

It is in the range of expected values for real gases at low pressures as calculated from the ratio of specific heats, C_p/C_V about 1.2 to 1.5. Also in Figure 7, γ derived from the experimental adiabat rises from its C-J value to a maximum of 5.63 at $V = 1.06$ cm^3/g, then decreases to 5.53 at $V = 1.15$ cm^3/g. The use of the empirical equation, $P(V + V^*) = G_2$ for $V > 1.15$ cm^3/g produces a discontinuity in $-\left(\frac{\partial \log P}{\partial \log V}\right)_S$ as indicated by the broken line in Fig. 7.

V. REFERENCES

1. W. E. Deal, "Measurements of the Reflected Shock Hugoniot and Isentrope for Explosive Reaction Products", Phys. of Fluids, 1, 523 (1958).

2. W. Fickett and W. W. Wood, "Detonation-Product Equation of State Obtained from Hydrodynamic Data", Phys. of Fluids, 1, 528 (1958).

3. J. W. S. Allan and B. D. Lambourn, "An Equation of State of Detonation Products at Pressures Below 30 kbars", 4th Symp. on Det., 52 (1965).

4. T. P. Liddiard and B. E. Drimmer, "J. Soc. Motion Picture and Tele. Engrs., 70, 106 (1961).

5. D. Price, "Contrasting Patterns in the Behavior of High Explosives", 11th Symp. on Comb., 1967, The Combustion Inst., Pitts., Pa.

6. H. Eyring, R. E. Powell, G. H. Duffey, and R. B. Parlin, "The Stability of Detonation", Chem. Rev., 45, 69 (1949).

7. W. W. Wood and J. G. Kirkwood, "Diameter Effect in Condensed Explosives. The Relation Between Velocity and Radius of Curvature of the Detonation Wave", J. Chem. Phys., 22, 1920-24 (1954).

8. M. A. Cook, G. S. Horsky, R. T. Keyes, W. A. Partridge, and W. O. Ursenback, "Detonation Wave Fronts in Ideal and Non-ideal Detonation", J. Appl. Phys., 27, 269 (1956).

9. R. E. Duff and E. Houston, J. Chem. Phys., 23, 1268 (1955), report the spike region is about 1 mm in aluminum impacted by Composition B with a reaction zone thickness of 0.13 mm.

10. See N. L. Coleburn, "The Compressibility of Pyrolytic Graphite", J. Chem. Phys., 40, 71 (1964). Also N. L. Coleburn and T. P. Liddiard, "The Unreacted Shock Hugoniots of Several Explosives", ibid, 44, 1929 (1966).

11. J. Hilsenrath and M. Klein, "Table of Thermodynamic Properties of Air in Chemical Equilibrium Including Second Virial Corrections from 1500°K to 15,000°K", AEDC-TDR-63-16 (August 1963); also, J. Hilsenrath and M. Klein, "Tables of Thermal Properties of Air", NBS Circ. 564, Wash., D. C. (1953).

12. R. H. Christian, R. E. Duff, and F. Yarger, "Shock Hugoniot of Argon", J. Chem. Phys., 23, 2042 (1955).

13. J. W. Bond, Jr., Los Alamos Rpt. LA-1693 (unpublished). J. W. Bond, Jr., "Structure of Shock Front in Argon", Phys. Rev., 105, 1683 (1957).

14. This assumption is supported for high charge densities by the experimental data of A. N. Dremin, P. F. Pokhil, M. I. Arifov, AKAD. NAUK. (DOKL.), 131, 5 (1960), (in Russian).

15. H. Jones, 3rd Symp. on Comb., Flame and Explosion Phenomena, Williams and Wilkins, Balto., Md., p. 590 (1949).

16. R. G. McQueen and S. P. Marsh, J. Appl. Phys., 31, 1253 (1960).

17. M. H. Rice, R. G. McQueen, and J. M. Walsh, "Compression of Solids by Strong Shock Waves", Solid State Physics, Vol. 6, edited by F. Seitz and D. Turnbull, Academic Press, Inc., New York (1958).

18. N. L. Coleburn, "The Dynamic Compressibility of Solids from Single Experiments Using Light-Reflection Techniques", NAVWEPS Rpt. 6026 (31 Oct. 1960).

19. M. H. Rice and J. M. Walsh, J. Chem. Phys., 26, 824 (1957).

20. Shock velocity and free-surface velocity of polyurethane were measured from 14.6 mm to 3.4 mm thickness, then assumed constant to zero thickness.

TABLE I

PARTICLE VELOCITY VS THICKNESS DATA

Material	Thickness (mm)	u* (cm/μsec)
Brass	24.2	.065
ρ_o = 8.40 g/cm^3	24.1	.066
	19.0	.068
	18.0	.069
	17.0	.071
	16.1	.071
	15.0	.071
	12.7	.074
	11.0	.075
	10.5	.075
	10.0	.075
	7.62	.077
	7.11	.076
	6.22	.078
	4.83	.078
Aluminum	25.0	.118
ρ_o = 2.74 g/cm^3	25.0	.119
	12.3	.130
	10.0	.133
	8.0	.133
	7.0	.134
	6.4	.135
	5.0	.135
	3.2	.137
Plexiglas	12.0	.212
ρ_o = 1.18 g/cm^3	10.1	.218
	9.5	.225
	8.5	.239
	7.25	.244
	5.50	.243
	5.00	.249
	4.50	.239
	4.25	.243
	4.00	.242
	3.50	.239
	3.00	.243
Polyurethane	14.6	.237
ρ_o = 0.188 g/cm^3	14.4	.284
	6.45	.297
	3.38	.325

*u = $\frac{\text{Free-surface velocity}}{2}$

TABLE II

PRESSURE-PARTICLE VELOCITY MEASUREMENTS

Material	ρ_o (g/cm^3)	P_o (bars)	P(kbars)	u(cm/μsec)	U(cm/μsec)
Brass[16]	8.40	----	338	0.080	0.503
Aluminum[17]	2.74	----	270	0.137	0.719
Plexiglas[18]	1.18	----	181.0	0.243	0.630
Water[19]	1.00	----	156.4	0.262	0.597
Polyurethane[20]	0.188	----	37.9	0.325	0.620
Argon	7.05×10^{-2}	40.8	16.9	0.450	0.534
"	4.7×10^{-2}	27.0	11.8	0.462	0.545
"	3.09×10^{-2}	17.9	7.92	0.466	0.550
"	1.55×10^{-2}	9.0	4.70	0.510	0.594
"	1.02×10^{-2}	6.0	3.39	0.537	0.621
Air	7.10×10^{-3}	6.0	2.54	0.570	0.627
"	3.55×10^{-3}	3.0	1.41	0.602	0.660
"	3.55×10^{-3}	3.0	1.46	0.613	0.672
"	3.43×10^{-3}	3.0	1.30	0.587	0.645
"	1.27×10^{-3}	1.0	0.67	0.697	0.761
"	1.27×10^{-3}	1.0	0.67	0.692	0.756
"	8.9×10^{-4}	0.7	0.51	0.723	0.794
"	6.3×10^{-4}	0.5	0.37	0.727	0.793
"	6.3×10^{-4}	0.5	0.37	0.730	0.796
"	3.7×10^{-4}	0.3	0.26	0.805	0.875
"	3.6×10^{-4}	0.3	0.23	0.764	0.832
"	12.6×10^{-5}	0.1	0.101	0.860	0.933
"	12.6×10^{-5}	0.1	0.101	0.860	0.933
"	8.86×10^{-5}	0.07	0.069	0.848	0.920
"	8.01×10^{-5}	0.07	0.069	0.890	0.965
"	1.23×10^{-5}	0.01	0.015	1.054	1.138
"	1.23×10^{-5}	0.01	0.015	1.070	1.155
"	1.23×10^{-5}	0.01	0.016	1.104	1.191

* See designated references for the Hugoniot equation-of-state of material. Free-surface velocities (=2u) of solid materials were obtained by extrapolation of the data in Table I to zero material thickness. Initial shock velocities were measured for water, air, and argon.

TABLE III

EQUATION-OF-STATE CONSTANTS FOR HBX-1

ρ	=	1.712 g/cm³
ρ_o	=	1.624 g/cm³
D	=	7.307 mm/μsec
γ_{CJ}	=	2.934
P_{CJ}	=	220.4 kbar
u_{CJ}	=	1.858 mm/μsec
ρ_{CJ}	=	2.178 g/cm³
$\frac{dD}{d\rho_o}$	=	3800 $\frac{m}{sec}/\frac{g}{cm^3}$
α	=	0.1325
W	=	0.3432
V_C	=	1.15 cm³/g
P_C	=	3.645 kbar
k	=	6.45 g/cm³
B	=	4.187 Mbar
G_1	=	0.00397 Mbar
G_2	=	9.142 x 10^9 (cm/sec)²
V*	=	1.358 cm³/g
M	=	-10.4799 μsec/cm

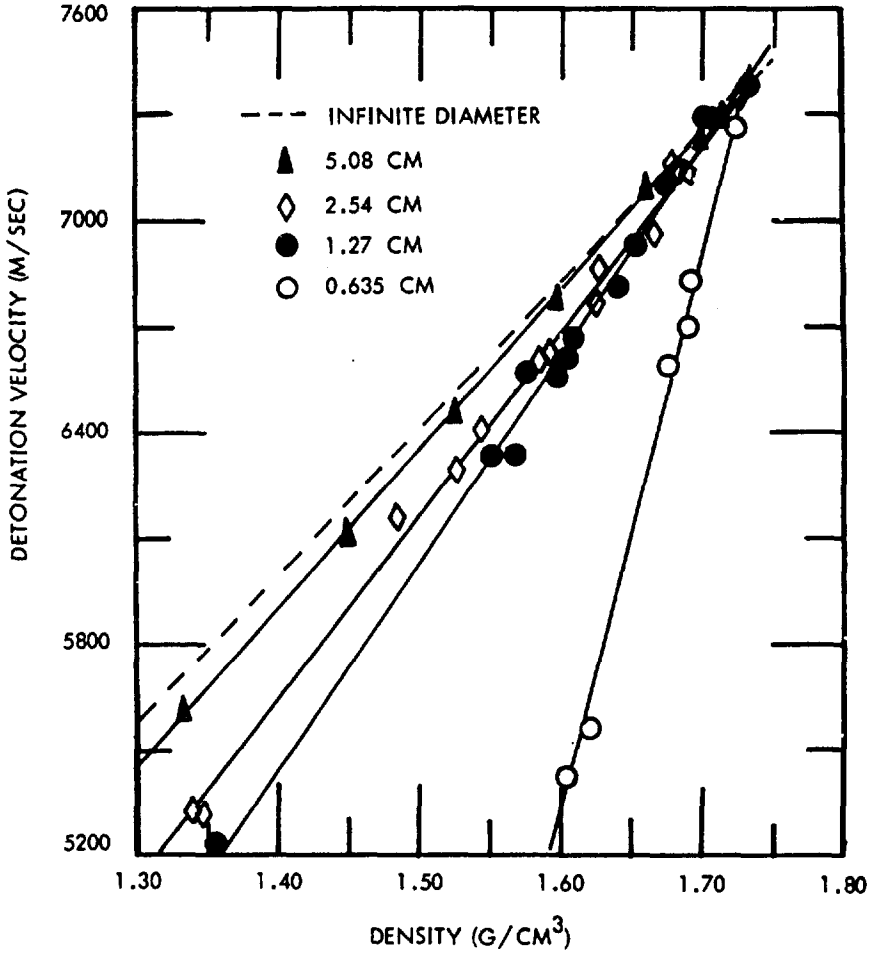

FIG. 1 DETONATION VELOCITY VS DENSITY FOR SEVERAL CHARGE DIAMETERS OF PRESSED HBX-1

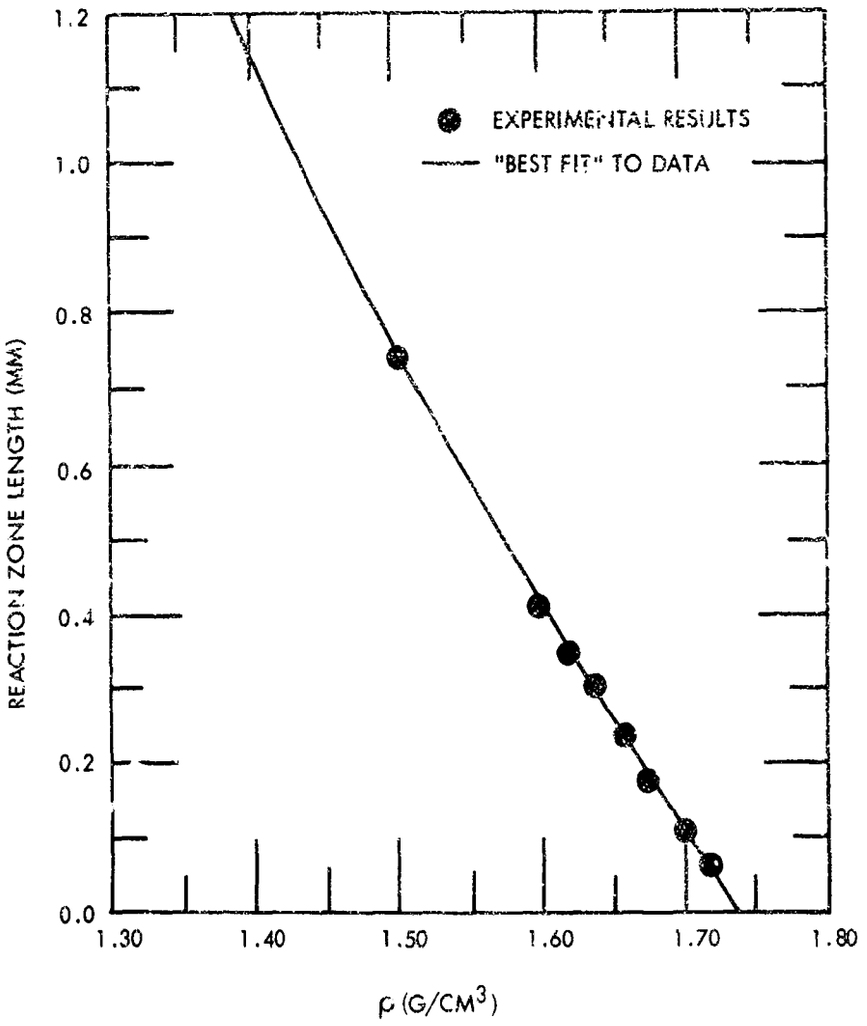

FIG. 2 REACTION ZONE LENGTH VS DENSITY OF PRESSED HBX-1

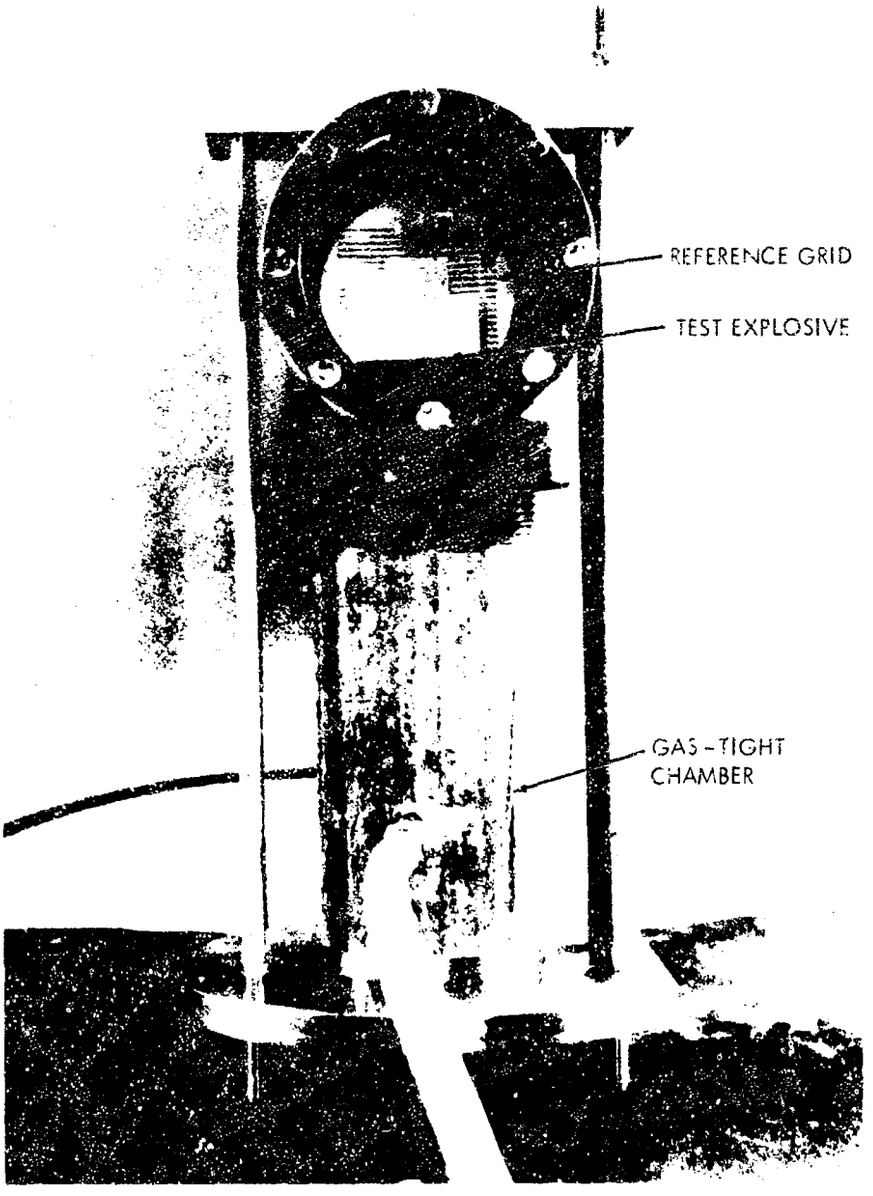

FIG. 3 TEST CHAMBER FOR SHOCK MEASUREMENTS IN GASES

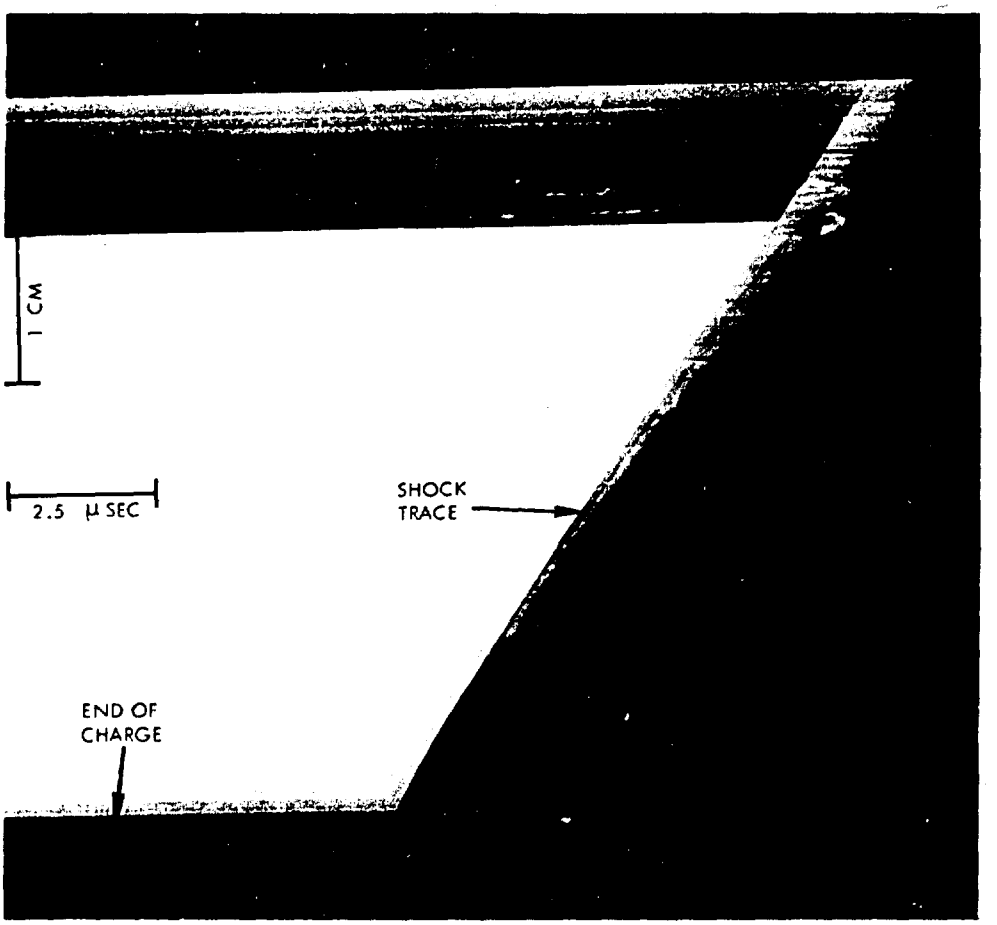

FIG. 4 SMEAR CAMERA RECORD OF SHOCK WAVE PROPAGATION FROM THE END OF AN HBX-1 CYLINDER

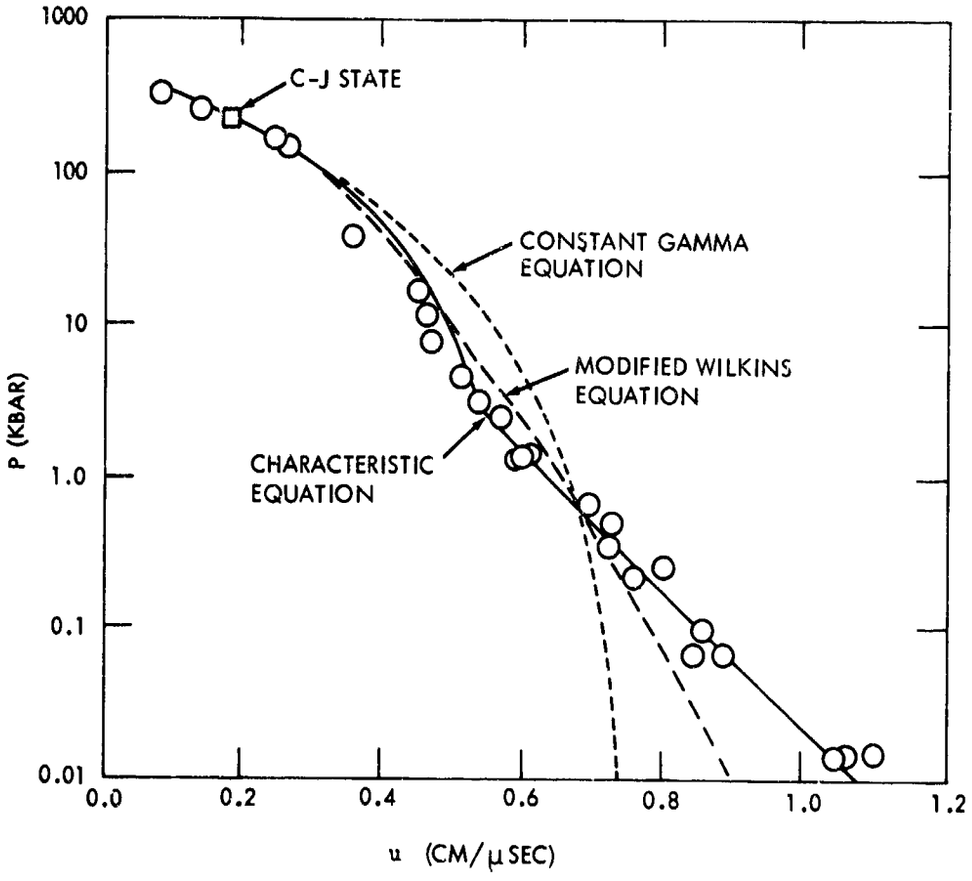

FIG. 5 EXPERIMENTAL PRESSURE - PARTICLE VELOCITY DATA AND EQUATION - OF - STATE RESULTS FOR PRESSED HBX-1

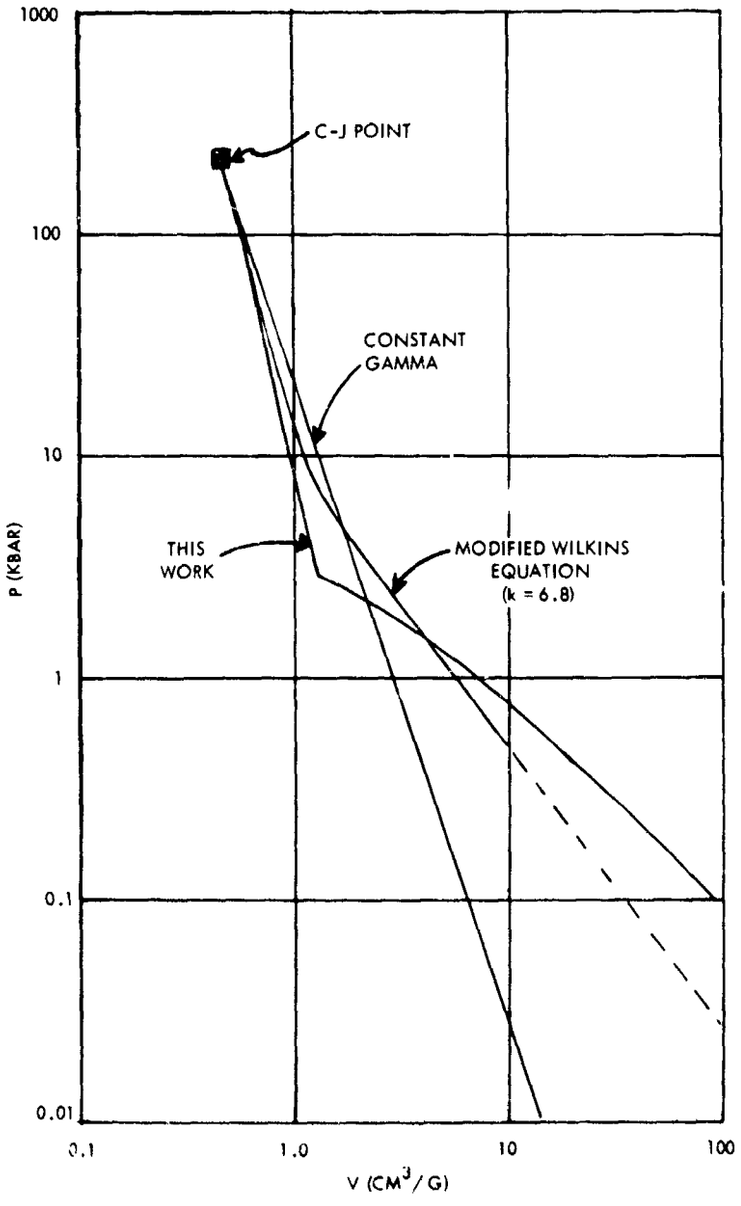

FIG. 6 PRESSURE - VOLUME ADIABATS FOR HBX-1

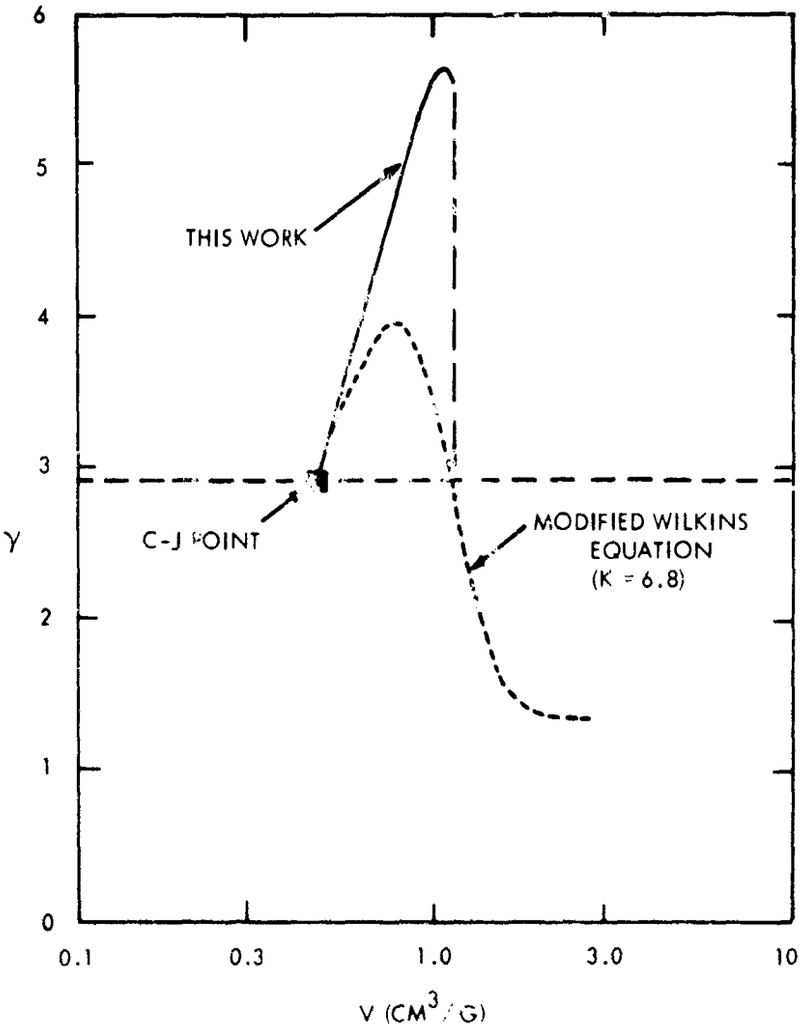

FIG. 7 VARIATION OF $\gamma = -\left(\frac{\partial \log P}{\partial \log V}\right)_S$ WITH VOLUME OF REACTION PRODUCTS FROM HBX-1

UNCLASSIFIED

Security Classification

DOCUMENT CONTROL DATA - R & D

Security classification of title, body of abstract and indexing annotation must be entered when the overall report is classified)

1. ORIGINATING ACTIVITY (Corporate author) U. S. Naval Ordnance Laboratory White Oak, Silver Spring, Maryland 20910	2a. REPORT SECURITY CLASSIFICATION UNCLASSIFIED 2b. GROUP

3. REPORT TITLE

Hydrodynamic Behavior of HBX-1 and Equation of State of the Detonation Products Below the Chapman-Jouguet State

4. DESCRIPTIVE NOTES (Type of report and inclusive dates)

5. AUTHOR(S) (First name, middle initial, last name)

Leslie A. Roslund and Nathaniel L. Coleburn

6. REPORT DATE	7a. TOTAL NO. OF PAGES	7b. NO. OF REFS
6 November 1970	16	15

8a. CONTRACT OR GRANT NO b. PROJECT NO ORD 332 001/UF17 354 315 p201 c. d.	9a. ORIGINATOR'S REPORT NUMBER(S) NOLTR 70-133 9b. OTHER REPORT NO(S) (Any other numbers that may be assigned this report)

10. DISTRIBUTION STATEMENT

This document has been approved for public release and sale, its distribution is unlimited.

11. SUPPLEMENTARY NOTES	12. SPONSORING MILITARY ACTIVITY Naval Ordnance Systems Command

13. ABSTRACT

The stability to detonation and the expansion behavior of reaction products were studied for an aluminized explosive, HBX-1. The detonation velocity-charge diameter and detonation velocity-loading density relationships were determined by streak camera techniques and electronic probe methods. These data gave reaction zone lengths which increase from 0.07 mm for an initial explosive density of 1.72 g/cm^3 to 1.5 mm at 1.3 g/cm^3. With the pressure-particle velocity relation established from 338,000 bars to 15 bars, and conditions in the C-J state (P_{CJ} = 220.4 kbars) specified, the generalized hydrodynamic relations derived by Jones were used to evaluate the constants in an empirical equation of state and in the Wilkins equation of state as modified by Allan and Lambourn.

DD FORM 1 NOV 65 1473 (PAGE 1)

S/N 0101-807-6801

UNCLASSIFIED

Security Classification

14 KEY WORDS	LINK A		LINK B		LINK C	
	ROLE	WT	ROLE	WT	ROLE	WT
High Explosives						
HBX-1						
Aluminized Explosives						
Reaction Zone Length						
Failure Diameter						
Explosive Effects						
Detonation Product Expansion						